phys. stat. sol. (b) **235**, No. 2, 238–247 (2003) / **DOI** 10.1002/pssb.200301563

Nonlinear polarization in nitrides revealed with hydrostatic pressure

G. Vaschenko[*,1], **C. S. Menoni**[1], **D. Patel**[1], **C. N. Tomé**[2], **B. Clausen**[2], **N. F. Gardner**[3], **J. Sun**[3], **W. Götz**[3], **H. M. Ng**[4], and **A. Y. Cho**[4]

[1] Colorado State University, Fort Collins, CO 80523, USA
[2] MST Division, Los Alamos National Laboratory, Los Alamos, NM 87545, USA
[3] LumiLeds Lighting, 370 W. Trimble Road, San Jose, CA 95131, USA
[4] Bell Laboratories, Lucent Technologies, 600 Mountain Avenue, Murray Hill, NJ 07974, USA

Received 5 August 2002, revised 30 August 2002, accepted 30 August 2002
Published online 4 February 2003

PACS 77.65.Bn, 77.65.Ly, 78.55.Cr, 78.66.Fd

We use hydrostatic pressure as an instrument to reveal a strong nonlinearity of the electrical polarization in group-III nitride quantum well structures. From the photoluminescence peak energies of the quantum well emission at different applied pressures we obtain the values of the built-in electric field in the wells and the corresponding well-barrier polarization difference. We found that in both the InGaN/GaN and GaN/AlGaN systems the field and the polarization difference increase with pressure much faster than expected from the conventional (linear) model of polarization. This behavior is explained by the dramatic strain dependence of the piezoelectric coefficients of the group-III nitrides, which constitutes the nonlinear piezoelectric effect.

Introduction The electrical polarization that exists in the nitrides due to the low symmetry of the wurtzite crystal lattice has a great impact on the electrical and optical properties of the heterostructures composed of these materials. Polarization induces an electrical field across the layers of the heterostructures with magnitudes in excess of 5 MV/cm [1]. The fields of such magnitude may significantly shift the emission peak of the light emitting diode or laser, increase the laser threshold current [1], or produce a high concentration two-dimensional electron gas in a transistor structure [2]. To design these and other nitride based devices in a controllable fashion one needs to be able to describe quantitatively the polarization and the built-in electric fields.

The conventional model of macroscopic polarization in nitrides is based on the assumption that the electromechanical properties of these materials are essentially linear with applied strain ε and electric field E [1–3]. Such an assumption is accurate only for an infinitesimal strain and field, a condition that is very unlikely in the nitride structures notorious for the large lattice mismatch strains and large built-in electric fields. The electromechanical interactions at fixed temperature in any material can be described as [4, 5]:

$$P_i = P_i^{sp} + e_{ij}\varepsilon_j + \epsilon_0\chi_{ik}E_k + 1/2e_{jil}\varepsilon_l\varepsilon_j + 1/2\epsilon_0\chi_{ikm}E_m E_k + f_{ikj}E_k\varepsilon_j + \ldots \quad (1)$$

and

$$\sigma_j = C_{ji}\varepsilon_l - e_{ij}E_i + 1/2C_{jln}\varepsilon_l\varepsilon_n - e_{ijl}E_i\varepsilon_l - 1/2\,f_{jik}E_iE_k + \ldots , \quad (2)$$

* Corresponding author: e-mail: vaschen@engr.colostate.edu, Phone: +1 970 491 8426

 0370-1972/03/23502-0238 $ 17.50+.50/0

where P_i, P_i^{sp}, and E_i are the components of the total polarization, spontaneous polarization, and electric field intensity vectors; ε_j and σ_j are the strain and stress components; e_{ij}, χ_{ik}, and C_{jl} are the piezoelectric coefficients, dielectric susceptibilities, and elastic stiffness coefficients; ϵ_0 is the permittivity of free space; e_{jil}, χ_{ikm}, f_{ikj}, and C_{jln} are the nonlinear electromechanical coefficients. The last three terms in Eqs. (1) and (2) introduce six second order effects which can be identified (in the order of their appearance in the equations) as nonlinear piezoelectricity $e(\varepsilon)$, electrooptical effect $\chi(E)$, photoelastic effect $\chi(\varepsilon)$, nonlinear elasticity $C(\varepsilon)$, electroelastic effect $C(E)$, and electrostriction $e(E)$. Until now very little is known about the magnitude of these effects in nitrides. Shimada et al. [6] predicted, based on Berry phase calculations, a strong dependence of the piezoelectric coefficients of AlN, GaN and BN on the volume conserving (deviatoric) strain. Guy et al. [7] suggested strong nonlinear piezoelectric effect in GaN from the experimental observations of the electrostriction in this material. More recently Bernardini and Fiorentini [8] performed calculations of the nonlinear piezoelectric response to the lattice mismatch strain in nitrides. Kato and Hama [9] explored nonlinear elasticity in AlN by calculating the pressure dependence of the elastic stiffness coefficients. This dependence was experimentally studied by Gerlich et al. [10]. The electrooptical and photoelastic effects in some of the group-III nitrides have also been investigated [11–13].

In this contribution we provide experimental evidence of a nonlinear pressure response of macroscopic polarization in the group-III nitrides and through the analysis of the secondary effects show that this nonlinearity mainly arises from changes in the piezoelectric coefficients with strain. To reveal the nonlinear behavior of the polarization we investigate the pressure dependent photoluminescence (PL) from InGaN/GaN and GaN/AlGaN quantum wells (QWs). The stress produced by pressure induces a polarization change in the layers of the QW structures that results in the increase of the built-in electric field. The analysis of the PL peak energies at different pressures suggests that the electric field increases by 0.32–1.2 MV/cm in the pressure range of 9 GPa. This increase is significantly larger than that obtained from the calculations based on linear model of polarization (0.11–0.46 MV/cm). On the other hand, the change in the built-in field and polarization is found to be in reasonable agreement with models of polarization taking into account nonlinear piezoelectricity.

Experiment The InGaN/GaN QW structures studied in this work were grown by metal-organic chemical vapor deposition on (0001) sapphire substrates. The InN mole fraction in the wells was ~0.15. Three different samples had each four wells 2.5 nm, 3.1 nm, and 3.8 nm thick, respectively, and 12.5 nm GaN barriers. The quantum well regions were deposited on 3.5 μm GaN layers.

The GaN/AlGaN structures were prepared by plasma assisted molecular beam epitaxy also on (0001) sapphire. Three samples investigated in this work had similar geometry with 5.2 nm AlGaN barriers and a combination of four GaN wells 1.8 nm, 2.9 nm, 3.9 nm, and 4.9 nm thick. The AlN mole fraction x in the barriers of different samples was 0.2, 0.5, and 0.8, respectively. The QW structures were grown on 0.6–0.8 μm GaN layers. All samples investigated in this work were nominally undoped.

To apply hydrostatic pressure, (70 × 70 × 30) μm^3 samples were loaded in a standard gasketed diamond anvil cell filled with liquid argon. Pressure was calibrated with the R_2 ruby crystal emission line. Pressure was increased at room temperature, while the measurements were done at 35 K. The PL was excited by the third harmonic of a mode-locked Ti:sapphire laser at 270 nm. The PL emission was collected in a backscattering geometry and detected with a 0.25 m spectrometer and liquid nitrogen cooled charge coupling device (CCD) camera. Time resolved measurements with resolution of ~0.8 ns were obtained with a fast photomultiplier tube and digital oscilloscope in accumulation mode.

Experimental results Figure 1a shows the pressure dependence of the PL peak energies in InGaN/GaN quantum wells and in the GaN at a low optical excitation of ~2 W/cm^2. The pressure coefficients (dE/dp) of the QW PL peaks are smaller than that of the GaN and show a clear trend with respect to well width: they decrease from 18.9 meV/GPa in the 2.5 nm wells to 1.6 meV/GPa in the 3.8 nm wells. Also, the pressure coefficients of the QW PL peaks increase as the optical excitation intensity is

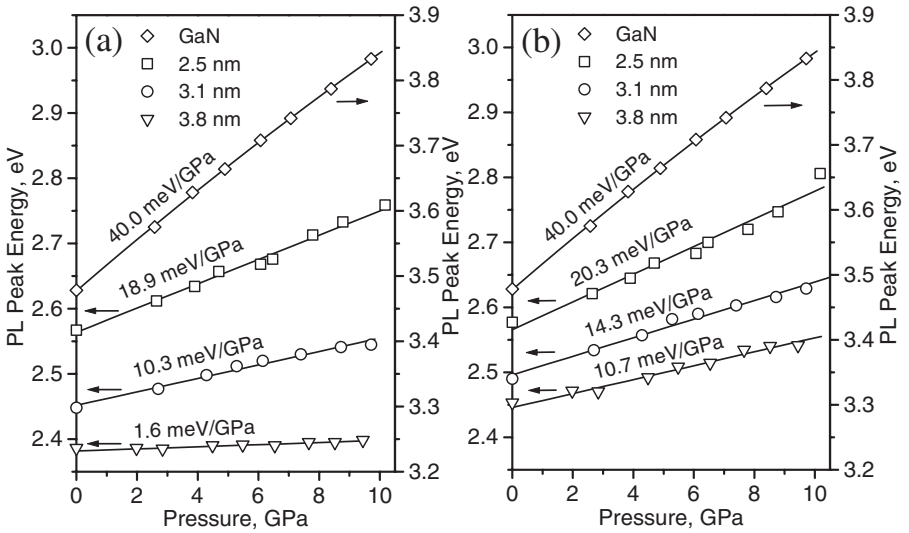

Fig. 1 Pressure dependence of the PL peak energies in InGaN/GaN QWs at optical excitation intensity of a) 2 W/cm^2, and b) 200 W/cm^2. The lines are the fits to the data points; the numbers show d*E*/d*p*'s.

increased from ~2 W/cm^2 (Fig. 1a) to ~200 W/cm^2 (Fig. 1b), the increase being more pronounced in the wider wells.

In the GaN/AlGaN structures we observe qualitatively similar pressure behavior as in InGaN/GaN, agreeing with the results of Łepkowski et al. [14] for GaN/$Al_{0.17}Ga_{0.83}N$ QWs. Figure 2 shows the pressure dependence of the QW PL peaks in the samples with $x = 0.5$ (a) and $x = 0.8$ (b). The pressure coefficient reduces from 26.2 (16.1) meV/GPa in the 1.8 nm well to only 2.9 (−7.2) meV/GPa in the 4.9 nm well in the sample with $x = 0.5$ (0.8). The negative pressure coefficient observed in the 4.9 nm well of the sample with $x = 0.8$ is a rather outstanding result, as it is a very uncommon pressure behavior of QW PL.

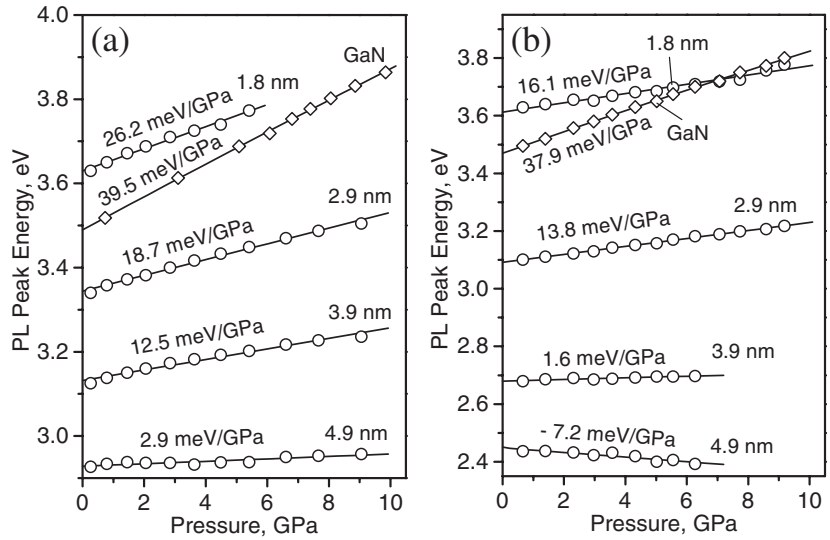

Fig. 2 Pressure dependence of the PL peak energies in GaN/AlGaN QWs at optical excitation intensity of 2 W/cm^2 in samples with AlN mole fraction in the barriers of a) 0.5, and b) 0.8.

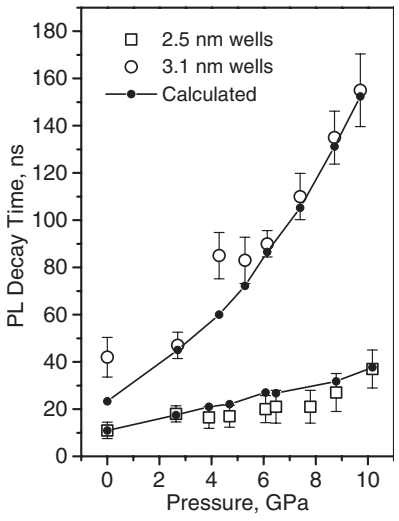

Fig. 3 Pressure dependence of the PL decay time in InGaN/GaN QWs at optical excitation intensity of 2 W/cm^2. The solid lines show the carrier lifetime change calculated with the experimentally determined E_w.

Figure 3 shows the pressure dependence of the PL decay time in the InGaN/GaN sample. The decay time, which was measured in a spectral interval within 20 meV from the PL peaks, significantly increases with pressure. This effect is especially evident in the structure with wider wells where the decay time increases by a factor of four. The significant increase of the decay time with pressure was also observed in the GaN/AlGaN structures.

Discussion and analysis The peculiar pressure behavior observed in our QW structures can be explained by the modification of the polarization in the wells and in the barriers by the pressure induced strain, which leads to a significant increase of the built-in electric field E_w in the wells [15, 16]. By virtue of the quantum confined Stark effect [17] the electric field increase produces a red shift of the emission peaks approximately described by $q\Delta E_w L_w$, where q is the electron charge and L_w is the well width. This shift competes with the strain induced blue shift in the band gap of the quantum well material, effectively reducing dE/dp; the effect being stronger in the wide wells. When we increase the optical excitation the large concentration of the photogenerated charge carriers partially screens out the built-in electric field. Therefore the field-induced shift reduces and the pressure coefficient of PL peak increases (Fig. 1b).

The decay time increase with pressure is also explained by the increase of the built-in electric field. We note that in the absence of the field the radiative lifetime in the QWs is not expected to change significantly with pressure. This is confirmed experimentally by the observed slight reduction of the decay time in a thick InGaN epilayer [18], where the electric field is not important due to self screening effect [1]. The increase of the decay time observed in the quantum wells is therefore exclusively due to the spatial separation of the electrons and holes in the quantum wells leading to a reduced overlap of their wavefunctions. The decay times of the InGaN/GaN QWs obtained here are a measure of the radiative processes dominating over the nonradiative ones as follows from the experimentally observed invariance of the integrated PL intensity with pressure.

To support our qualitative explanation of the pressure behavior of the QW PL peak energy and decay time and to obtain the magnitudes of the built-in electric field and polarization we have analyzed the experimental data by calculating the strain in the quantum well and barrier layers of the InGaN/GaN structure and then determining the shift of the PL peaks using the deformation potentials of GaN and InGaN. To find the strain in the InGaN QWs we add to the lattice mismatch strain a strain generated by the applied pressure. In these calculations we assume that the lattice mismatch between the GaN buffer and the sapphire substrate is accommodated by the low temperature grown nucleation layer, and therefore the buffer is essentially strain free before we apply pressure [19, 20]. Also, since the GaN buffer layer is much thicker than the QW layers we assume that most of the lattice mismatch between the GaN and InGaN is accommodated by the latter. With these assumptions the in-plane elastic strain in the wells is $\varepsilon_1^{\text{mism}} = \varepsilon_2^{\text{mism}} = (a_{\text{GaN}} - a_{\text{InGaN}})/a_{\text{InGaN}}$, where a_{GaN} = 3.189 Å and a_{InGaN} = 3.241 Å are the lattice constants of free-standing GaN and InGaN films [21].

The sapphire substrate is the thickest element of the whole structure. Therefore the in-plane deformation of the samples with applied pressure is controlled by this element, resulting in equal pressure induced strains in the substrate, GaN, and InGaN layers [19]. To calculate these strains we assume a quasi-

hexagonal symmetry of the substrate. This can be justified since the elastic stiffness coefficient of sapphire C_{14} = –23 GPa is almost an order of magnitude smaller than the other elements of the stiffness tensor of this material [22]. Applying Hooke's law the pressure generated in-plane strain can be written as

$$\varepsilon_1^{\mathrm{p}} = \varepsilon_2^{\mathrm{p}} = \frac{C_{13} - C_{33}}{(C_{11} + C_{12})\, C_{33} - 2C_{13}^2}\, p\,, \tag{3}$$

where C_{ij} are the elastic stiffness coefficients of sapphire, and p is the applied pressure in GPa. The total in-plane strain in the wells $\varepsilon_{1,2}^{\mathrm{w}}$ and in the barriers $\varepsilon_{1,2}^{\mathrm{b}}$ is given by

$$\varepsilon_1^{\mathrm{w}} = \varepsilon_2^{\mathrm{w}} = \varepsilon_1^{\mathrm{mism}} + \varepsilon_1^{\mathrm{p}}\,; \qquad \varepsilon_1^{\mathrm{b}} = \varepsilon_2^{\mathrm{b}} = \varepsilon_1^{\mathrm{p}}\,. \tag{4}$$

The strain in the growth direction in the barriers $\varepsilon_3^{\mathrm{b}}$ and in the wells $\varepsilon_3^{\mathrm{w}}$ can be found from Hooke's law considering continuity of stress $\sigma = -p$:

$$\varepsilon_3^{\mathrm{b}} = \frac{-p - 2C_{13}^{\mathrm{GaN}}\varepsilon_1^{\mathrm{p}}}{C_{33}^{\mathrm{GaN}}}\,; \tag{5}$$

$$\varepsilon_3^{\mathrm{w}} = -2\frac{C_{13}^{\mathrm{InGaN}}}{C_{33}^{\mathrm{InGaN}}}\,\varepsilon_1^{\mathrm{mism}} + \frac{-p - 2C_{13}^{\mathrm{InGaN}}\varepsilon_1^{\mathrm{p}}}{C_{33}^{\mathrm{InGaN}}} = \varepsilon_3^{\mathrm{mism}} + \varepsilon_3^{\mathrm{p}}\,. \tag{6}$$

The terms proportional to C_{13}/C_{33} in Eqs. (5) and (6) account for the Poisson effect induced by the in-plane strain. The elastic stiffness coefficients of GaN and InN were obtained from Refs. [23] and [24] respectively. The InGaN coefficients were then obtained using linear interpolation.

The change of the InGaN band gap with applied pressure was estimated using the knowledge of the strain calculated from Eqs. (3) to (6) as [25]

$$\Delta E_{\mathrm{g}}^{\mathrm{InGaN}}(p) = 2\varepsilon_1^{\mathrm{p}}(a_{\mathrm{c}}^{\parallel} - D_2 - D_4) + \varepsilon_3^{\mathrm{p}}(a_{\mathrm{c}}^{\perp} - D_1 - D_3)\,, \tag{7}$$

where the deformation potentials for InGaN $a_{\mathrm{c}}^{\parallel} - D_2 = -9.18$ eV, $D_3 = 5.63$ eV, $a_{\mathrm{c}}^{\perp} - D_1 = -5.80$ eV, and $D_4 = -2.85$ eV were determined by linear interpolation between the theoretical values of the deformation potentials of GaN and InN [25]. Including the effects of the pressure dependence of the effective masses [26] and band offsets in the InGaN wells the band gap shift with pressure is found to be dE/dp = 38.2 meV/GPa. This value expected in the polarization free quantum wells of all thicknesses is confirmed by the dE/dp = 37.0 meV/GPa measured in an InGaN epilayer with InN mole fraction of 0.11 [18]. The small and well width dependent dE/dp of InGaN QW PL can not be explained by the effect of pressure on the band structure. The peculiar pressure behavior in these wells is therefore due to the modification of the built-in electric field with pressure.

When the built-in electric field across the wells is sufficiently large it almost exclusively defines the slope of the well width dependence of the PL peak energy in the wide QWs [27, 28]. This is the case in our InGaN/GaN samples as shown in Fig. 4a, where the linear fit to the atmospheric pressure PL peaks (solid line) is compared with that of the envelope-function calculation of the QW transitions (dashed line). Both fits provide the same value of the built-in electric field of 1.4 MV/cm, thus indicating that the E_{w} at each pressure can be found simply from the slopes of the PL peak energy/well width dependence [27]. These values of the electric field are shown in Fig. 4b. E_{w} increases from 1.4 MV/cm to 2.6 MV/cm when the pressure is increased to 9 GPa. To verify the values of E_{w} presented here we calculated how the radiative lifetime of QW PL would change with pressure as a result of increasing E_{w}. The lifetime variation was found from the inverse of the square of the electron-hole wavefunction overlap with E_{w} applied to the wells. The results of the calculations are shown in Fig. 3 by the solid lines. Good agreement be-

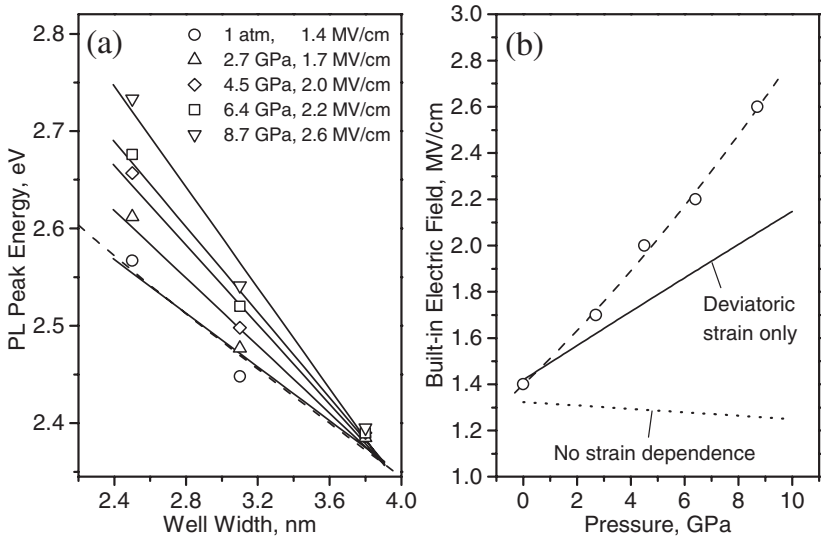

Fig. 4 a) Well width dependence of the PL peak energies in InGaN/GaN QWs at different applied pressures; b) the corresponding values of the built-in electric field (open symbols).

tween the measured decays and calculated lifetimes suggests that the values of E_w defined in this work are accurate.

Next we compared the values of E_w obtained from the experiment with those predicted by the linear model of polarization and by the work of Shimada et al. [6]. E_w can be estimated from [1]

$$E_w = (P_b - P_w)/(\epsilon_w + \epsilon_b L_w/L_b) , \tag{8}$$

where $\epsilon_{w,b}$ are the permittivities of the InGaN well and GaN barrier, $L_{w,b}$ are the well and barrier width, and $P_{b,w}$ are the total polarizations (spontaneous and piezoelectric) in the barriers and in the wells; the piezoelectric polarization components can be found as $P_{w,b}^{pz} = e_{33}^{w,b}\varepsilon_3^{w,b} + 2e_{31}^{w,b}\varepsilon_1^{w,b}$. The piezoelectric coefficients and the values of spontaneous polarization for InGaN and GaN were taken from Ref. [29]. The dotted line in Fig. 4b shows the change of E_w with pressure calculated within the framework of the linear model [1–3]. Instead of increase, this model predicts a slight reduction of the built-in field with pressure. This obvious contradiction between the linear model and experiment suggests the strong contribution of the secondary effects, such as nonlinear piezoelectricity, to the polarization response of our samples. To support this explanation we estimated the change of E_w considering the volume conserving strain dependence of the piezoelectric coefficients of GaN calculated by Shimada et al. [6]. Since the volume conserving strain dependence of the piezoelectric coefficients in InGaN is not available, we used for this material the strain dependence of GaN. The built-in field was then calculated in the same way as for the linear model. The solid line in Fig. 4b shows the result of this calculation. In this case the built-in field significantly increases with applied pressure, the slope of this increase being somewhat smaller than that observed in the experiment. This shows that nonlinear piezoelectricity can be responsible, at least in part, for the observed anomaly in the pressure behavior of the InGaN/GaN QWs. The underestimation of the calculated dependence can be attributed to the contribution of the dilatational strain not considered here, to the different strain dependence of the piezoelectric coefficients in InGaN than in GaN, or to the other secondary effects, such as nonlinear elasticity and photoelastic effect.

Obtaining an accurate description of the built-in electric field and polarization in the InGaN/GaN QW system is somewhat hindered by the uncertainty of the InGaN band gap energy and its pressure depen-

dence [30]. This is due to the uncertainty of the InN band gap energy itself, and due to the possible effects of the deformation potentials bowing and carrier localization [31]. In contrast, in the GaN/AlGaN QW system these effects are not expected to be important, and in analyzing the experimental results in this system we can use a more direct approach. To obtain the values of E_w in GaN/AlGaN QWs we fit the PL data with the model that describes e_1–hh_1 transition energy in the wells with the expression of the form $E_{e_1\text{–}hh_1} = E_{GaN} + E_{e_1} + E_{hh_1} - E_{ex}$, where E_{GaN} is the GaN band gap energy, E_{e_1} and E_{hh_1} are the electron and heavy hole confinement energies, and E_{ex} is the exciton binding energy. The GaN and AlGaN band energies at each pressure were found using the deformation potentials of GaN and AlN (the AlGaN deformation potentials were linearly interpolated from the values given for the binaries [25]). The confinement energies in the presence of E_w were found using the method described in Ref. [17]. The binding energies of the confined excitons subjected to E_w were found using the approach proposed by Leavitt and Little [32]. The only adjustable parameter in our model was the well-barrier polarization difference $P_w - P_b$, which essentially defines the built-in electric field in the wells as follows [33]:

$$E_w = \frac{-(P_w - P_b) + \rho}{\varepsilon(1 + L_w/L_b)} + \frac{V_s}{L_b + L_w} - \frac{qN_D}{\varepsilon}\left[d - \frac{L_b + L_w}{2}\right], \tag{9}$$

where ε is the permittivity of the GaN wells and AlGaN barriers (assumed here to be the same for the two materials, and independent of pressure), $L_{w,b}$ are the cumulative thicknesses of the well and the barrier layers, ρ is the two-dimensional photogenerated charge density in the wells that was estimated considering the measured decay times in different wells, V_s is the surface potential barrier determined as in Ref. [33], $N_D \approx 10^{17}$ cm^{-3} is the background doping concentration, and d is the distance from the barrier-buffer interface to the well where the field is to be calculated. Equation (9) describing the electric field in GaN/AlGaN QWs is different than that for the InGaN/GaN quantum wells (Eq. (8)) due to the proximity of the surface to the quantum well region in the former. The second and the third term in Eq. (9) essentially introduce surface effects into consideration.

Figure 5 shows the fits to the QW PL peak energies obtained with our model at an intermediate pressure of 5 GPa (solid lines). Good agreement between the fits and the experimental data suggests that the model accurately accounts for the effects responsible for shaping the QW PL peak energies. From the fits to the PL peaks at different pressures we obtain the pressure dependence of the $P_w - P_b$ and corresponding built-in electric field in 2.9 nm well in different samples. These results are shown by the open circles in Fig. 6. We found that in every sample the polarization difference significantly increases with pressure, which results in an increase of E_w by 0.32 MV/cm, 0.76 MV/cm, and 1.01 MV/cm in ~8 GPa in the samples with AlN mole fractions in the barriers of 0.2, 0.5, and 0.8, respectively. The increase is significantly larger than that predicted by the linear model of polarization (0.11, 0.26, and 0.46 MV/cm) shown by the solid lines in Fig. 6. This finding suggests that, as in the case of the InGaN/GaN wells, the linear model does not reproduce the pressure dependence of polarization in the GaN/AlGaN quantum wells.

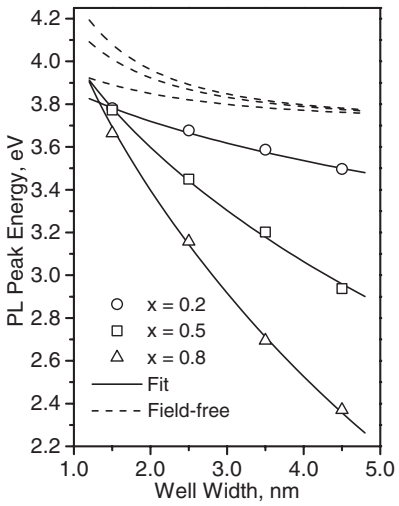

Fig. 5 Well width dependence of the PL peak energy in GaN/AlGaN QWs at 5 GPa. Open symbols are the experimental points; solid lines are the fits to the experimental data obtained with our model. The dashed lines are the QW transition energies calculated in the absence of the built-in electric field.

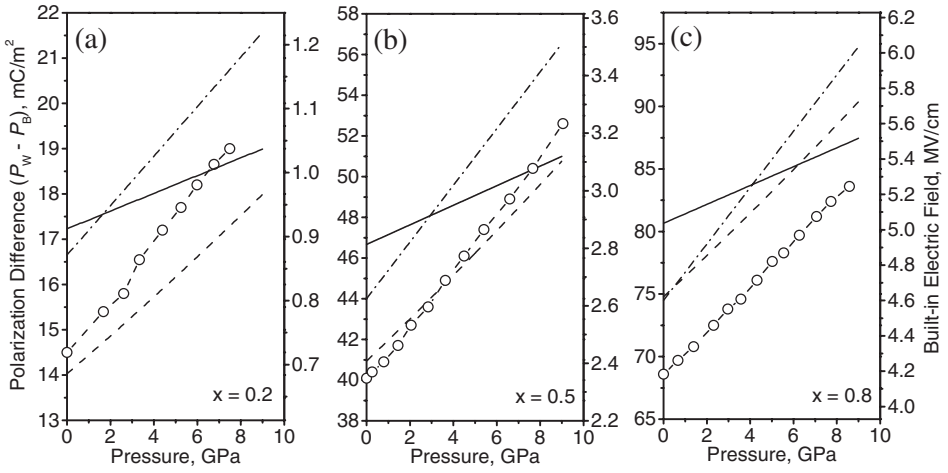

Fig. 6 Pressure dependence of $P_w - P_b$ and corresponding electric field in 2.9 nm GaN/AlGaN QWs with a) $x = 0.2$, b) $x = 0.5$, and c) $x = 0.8$. The experimental points were obtained from the fits to the PL data as shown in Fig. 5.

The dashed-dotted lines in Fig. 6 show the result of the calculation of the polarization difference where we introduce the volume conserving strain dependence of the GaN and AlGaN piezoelectric coefficients [6]. The slopes of these pressure dependences are significantly larger than those produced by the linear model and close to the slopes obtained from the experiment. We have also calculated the $P_w - P_b$ following the work on nonlinear polarization by Bernardini and Fiorentini [8]. We considered only the changes in piezoelectric polarization due to hydrostatic compression of the ideal crystal and due to the increase of the internal parameter u with pressure [34]. The resulting pressure dependences are shown by the dashed lines in Fig. 6. Using this model we again obtain slopes of $P_w - P_b$ close to the experimental ones. These findings suggest that as in the InGaN/GaN system the polarization response in GaN/AlGaN QWs is strongly affected by the strain dependence of the piezoelectric coefficients, i.e. by nonlinear piezoelectricity.

Now that we have shown that the nonlinear piezoelectricity plays the major role in defining the pressure behavior of PL in nitrides we can briefly analyze the possible contributions of the other secondary effects. In Figure 7 we recalculated the experimental and "linear" model values of $P_w - P_b$ introducing the nonlinear elasticity and photoelastic effect, for the GaN/AlGaN QWs with $x = 0.5$ (Fig. 6b). The nonlinear elasticity was taken into account by assuming pressure dependent elasticity coefficients C_{ij} of sapphire [35] and AlN [9]. The lack of reports on the pressure dependence of C_{ij} led us to assume for GaN the same dependence as in AlN. The effect of lattice mis-

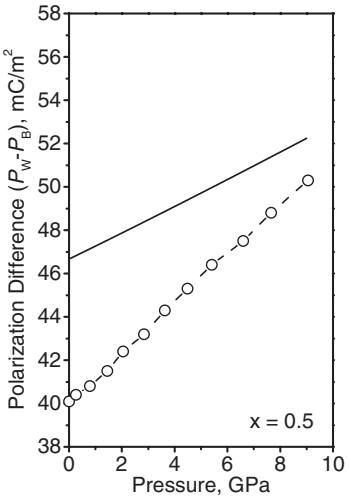

Fig. 7 Experimental (open circles) and model (solid line) pressure dependence of $P_w - P_b$ in the GaN/AlGaN QWs with $x = 0.5$ obtained considering pressure dependence of the elasticity coefficients C_{ij} of sapphire, AlN, and GaN, and that of the dielectric constants of AlN and GaN.

match strain was neglected (we found that it does not affect the slope of the pressure dependence). The pressure dependence of the electronic dielectric constants of GaN and AlN was taken from the Ref. [13]. As follows from these simple estimates the introduction of nonlinear elasticity and photoelastic effect, although producing tangible corrections to the polarization difference, does not have strong enough effect to explain the observed pressure response of polarization.

Conclusions We have presented clear experimental evidence of the nonlinear pressure response of the macroscopic polarization in group-III nitrides. The polarization change with pressure was evaluated using the pressure dependence of the PL peak energies in wells of varying width. The changes in polarization and built-in electric field are found to be comparable in magnitude with those predicted by the models of nonlinear piezoelectricity. Based on this finding and on the simple estimates of the possible contribution of other secondary effects we conclude that the strain dependence of the piezoelectric constants is mainly responsible for the polarization nonlinearity. The findings of this work reveal severe limitations of the conventional model of polarization in group-III nitrides.

References

[1] V. Fiorentini, F. Bernardini, F. Della Sala, A. Di Carlo, and P. Lugli, Phys. Rev. B **60**, 8849 (1999).
[2] O. Ambacher, J. Smart, J. R. Shealy, N. G. Weimann, K. Chu, M. Murphy, W. J. Schaff, L. F. Eastman, R. Dimitrov, L. Wittmer, M. Stutzmann, W. Rieger, and J. Hilsenbeck, J. Appl. Phys. **85**, 3222 (1999).
[3] A. D. Bykhovski, B. L. Gelmont, and M. S. Shur, J. Appl. Phys. **81**, 6332 (1997).
[4] W. P. Mason, Piezoelectric Crystals and their Application to Ultrasonics (D. Van Nostrand, New York, 1950), pp. 463–464.
[5] S. I. Chizhikov, N. G. Sorokin, and V. S. Petrakov, Ferroelectrics **41**, 9 (1982).
[6] K. Shimada, T. Sota, K. Suzuki, and H. Okumura, Jpn. J. Appl. Phys. **37**, L1421 (1998).
[7] I. L. Guy, S. Muensit, and E. M. Goldys, Appl. Phys. Lett. **75**, 3641 (1999).
[8] F. Bernardini and F. Fiorentini, Phys. Rev. B **64**, 085207 (2001).
[9] R. Kato and J. Hama, J. Phys.: Condens. Matter **6**, 7617 (1994).
[10] D. Gerlich, S. L. Dole, and G. A. Slack, J. Phys. Chem. Solids **47**, 437 (1986).
[11] J. Chen, Z. H. Levine, and J. W. Wilkins, Appl. Phys. Lett. **66,** 1129 (1995).
[12] J. L. P. Hughes, Y. Wang, and J. E. Sipe, Phys. Rev. B **55**, 13630 (1997).
[13] N. E. Christensen and I. Gorczyca, Phys. Rev. B **50**, 4397 (1994).
[14] S. P. Łepkowski, H. Teisseyre, T. Suski, P. Perlin, N. Grandjean, and J. Massies, Appl. Phys. Lett. **79**, 1483 (2001).
[15] G. Vaschenko, D. Patel, C. S. Menoni, N. F. Gardner, J. Sun, W. Götz, C. N. Tomé, and B. Clausen, Phys. Rev. B **64**, 241308 (2001).
[16] G. Vaschenko, D. Patel, C. S. Menoni, H. M. Ng, and A. Y. Cho, Appl. Phys. Lett. **80**, 4211 (2002).
[17] D. A. B. Miller, D. S. Chemla, T. C. Damen, A. C. Gossard, W. Wiegmann, T. H. Wood, and C. A. Burrus, Phys. Rev. B **32**, 1043 (1985).
[18] G. Vaschenko, D. Patel, C. S. Menoni, S. Keller, U. K. Mishra, and S. P. DenBaars, Appl. Phys. Lett. **78**, 640 (2001).
[19] P. Perlin, L. Mattos, N. A. Shapiro, J. Kruger, W. S. Wong, T. Sands, N. W. Cheung, and E. R. Weber, J. Appl. Phys. **85**, 2385 (1999).
[20] L. T. Romano, C. G. Van de Walle, J. W. Ager III, W. Götz, and R. S. Kern, J. Appl. Phys. **87**, 7745 (2000).
[21] M. Leszczynski, T. Suski, J. Domagala, and P. Prystawko, in: Properties, Processing and Applications of Gallium Nitride and Related Semiconductors, edited by J. H. Edgar, S. Strite, I. Akasaki, H. Amano, and C. Wetzel (INSPEC, London, 1999), p. 6.
[22] Y. Takeda and M. Tabuchi, in: Properties, Processing and Applications of Gallium Nitride and Related Semiconductors, edited by J. H. Edgar, S. Strite, I. Akasaki, H. Amano, and C. Wetzel (INSPEC, London, 1999), p. 381.
[23] A. Polian, M. Grimsditch, and I. Grzegory, J. Appl. Phys. **79**, 3343 (1996).
[24] A. F. Wright, J. Appl. Phys. **82**, 2833 (1997).
[25] W. W. Chow and S. W. Koch, Semiconductor-Laser Fundamentals (Springer, Berlin, 1999), pp. 189–191.
[26] P. Perlin, V. Iota, B. A. Weinstein, P. Wiśniewski, T. Suski, P. G Eliseev, and M. Osinski, Appl. Phys. Lett. **70**, 2993 (1997).

[27] R. André, J. Cibert, L. S. Dang, J. Zeman, and M. Zigone, Phys. Rev. B **53**, 6951 (1996).
[28] M. Leroux, N. Grandjean, J. Massies, B. Gil, P. Lefebvre, and P. Bigenwald, Phys. Rev. B **60**, 1496 (1999).
[29] F. Bernardini, F. Fiorentini, and D. Vanderbilt, Phys. Rev. B **63**, 193201 (2001).
[30] J. Wu, W. Walukiewicz, K. M. Yu, J. W. Ager III, E. E. Haller, H. Lu, W. J. Schaff, Y. Saito, and Y. Nanishi, Appl. Phys. Lett. **80**, 3967 (2002).
[31] P. Perlin, I. Gorczyca, T. Suski, P. Wisniewski, S. Lepkowski, N. E. Christensen, A. Svane, M. Hansen, S. P. DenBaars, B. Damilano, N. Grandjean, and J. Massies, Phys. Rev. B **64**, 115319 (2001).
[32] R. P. Leavitt and J. W. Little, Phys. Rev. B **42**, 11774 (1990).
[33] J. Simon, R. Langer, A. Barski, M. Zervos, and N. T. Pelekanos, phys. stat. sol. (a) **188**, 867 (2001).
[34] J.-M. Wagner and F. Bechstedt, Phys. Rev. B **62**, 4526 (2000).
[35] J. H. Gieske and G. R. Barsch, phys. stat. sol. **29**, 121 (1968).